Proceedings of the 17th World Congress
The International Federation of Automatic Control
Seoul, Korea, July 6-11, 2008

Towards Clean-Coal Control Technologies: Modelling Conversion of Carbon Oxide into Hydrogen by a Shift Reactor

S. Bittanti* S. Canevese A. De Marco*****
V. Prandoni D. Serrau******

**Dipartimento di Elettronica e Informazione (DEI), Politecnico di Milano, Piazza Leonardo Da Vinci 32, 20133, Milan, Italy (e-mail: sergio.bittanti@polimi.it)*
***CESI RICERCA, Via Rubattino 54, 20134, Milan, Italy (Tel: +39-02-3992-5696; e-mail: canevese@cesiricerca.it, prandoni@cesiricerca.it)*
****Consultant, Milan, Italy (e-mail: demarco@elet.polimi.it)*
*****Formerly student at DEI, Politecnico di Milano (e-mail: DanielaS@fastwebnet.it)*

Abstract: The operating behaviour of a catalytic reactor converting carbon oxide into hydrogen by water gas shift is analysed. Such a device can be used in coal gasification plants for hydrogen production. A dynamical model of the reactor is presented, based on a description of the kinetic-chemical mechanisms of adsorption and desorption in the porous catalyst and on mass, energy and momentum conservation equations. Chemical-kinetic parameters have been identified. The complete model has been validated against steady-state data gathered from a laboratory-scale reactor. Dynamical simulation results are shown as well.

1. INTRODUCTION

In an Integrated Gasification Combined Cycle (IGCC) plant, coal undergoes a gasification process yielding a synthetic gaseous fuel, the "syngas". The syngas can be employed either directly to feed the gas turbine of the combined cycle or to produce H_2. In this latter case, in order to extract as much hydrogen as possible, the syngas, first cleaned, is sent to a *shift process*, so that carbon monoxide is converted into hydrogen and carbon dioxide. The shift reactor is a critical component of the whole plant (Ogden, 1999). Here, we study this shift process, whose modelling is fundamental for control purposes. We make also reference to the shift reactor of an IGCC plant, with CO_2 capture and sequestration, currently under study at CESI RICERCA (Fantini *et al.*, 2007); in this plant, flexibility issues are also taken into account, so as to achieve the most convenient balance between electric energy and hydrogen production according to the markets constraints.

The paper is organised as follows: Section 2 describes the operating mechanisms of the catalytic shift process; in Section 3, a dynamical model, based on a thermo-fluid-dynamical and a kinetic-chemical description, for a single shift reactor is worked out; Section 4 deals with kinetic-chemical parameter identification and with model validation thanks to data from a laboratory facility; Section 5 reports some dynamical simulation results highlighting model reliability and predictive capabilities. It is believed that the model derived in this paper will be a major tool for the design of any control strategy, as hinted at in Section 6.

2. PROCESS DESCRIPTION

In the shift reactor, carbon monoxide is converted into hydrogen, thanks to the well-known Water Gas Shift reaction (WGSr):

$$CO + H_2O \leftrightarrow CO_2 + H_2\,,\ \Delta H = -41.1 \text{ kJ/kmol}\,.$$

The operating temperature of the feeding gas is rather low, namely around 610 K, so that equilibrium is shifted to the product side. However, the reaction can proceed only with a catalyst.

Schematically (see Figure 1), a shift fixed bed reactor is a metal cylinder filled with catalyst pieces, which can be thought of as small spheres. The feeding gas, which is composed mainly of H_2O, H_2, N_2, CO, CO_2, flows among the spheres and inside them, since they are highly porous; reactants in the feedgas are adsorbed in the porous medium, which acts as a catalyst for the WGSr and finally releases the reaction products. The main phenomena take place inside the porous medium and between the porous medium and the "bulk" gas flowing across the bed, according to the steps represented in Figure 2 (which is drawn from Yoon and Erickson, 2005):

1. *external diffusion*: reactants reach the outer surface of the catalyst pores, by crossing the limit layer by diffusion;

2. *internal diffusion*: reactants diffuse inside the catalyst pores;

3. *adsorption*: reactants are adsorbed by the catalyst;

4. *reaction*, according to its own kinetics;

5. *desorption*: products are desorbed from the catalyst surface;

6. *internal counterdiffusion*: products diffuse across pores until they reach the outer surface;

7. *external counterdiffusion*: products diffuse across the limit layer.

Phases 3, 4 and 5 are taken into account by the chemical kinetic model part, as described in Section 3.2, while the other phases can be included in the diffusive phenomena, so in a thermo-fluid-dynamical description (see Section 3.1), together with the description of the bulk gas flow.

3. MODELLING OF A SHIFT REACTOR

As already said, we consider a fixed bed of catalyst pellets through which the feeding gas mixture is sent, as shown in Figure 1, on the left part side. The gas flow feeding the reactor (the so-called *bulk flow*) is constituted by the syngas and water steam. Inside the reactor, gases penetrate, by diffusion, into the porous pellets, where adsorption and desorption of the various chemical species occur on the pores active surfaces, so that the shift reaction can develop. We assume that the system under study has cylindrical symmetry; let z and r be the reactor axial and radial coordinates, respectively. Since the dimensions of the porous pellets are much smaller than the reactor diameter and the reactor walls are adiabatic, the process variables related to the bulk flow are assumed to be uniform with respect to r. Besides, since the pellets can be represented by spheres, the fluid flux within them can be assumed with spherical symmetry. Therefore, the process variables on the sphere outer surface are uniform, and they are assumed to coincide with those of the bulk flow at the axial coordinate corresponding to the sphere position.

In order to build up a reliable and accurate thermo-fluid-dynamical model, first of all (Section 3.1), we write a distributed-parameter description, with reference to the bulk axial coordinate z and to the radial coordinate R of an ideal, typical, average sphere, of radius R_0. Such description will be completed by a kinetic-chemical description (Section 3.2).

3.1 Thermo-fluid-dynamical equations

In our description of the main phenomena taking place in the shift reactor, we will simply consider a gaseous bulk and a catalyst region. The former is a schematical representation of the gas flowing along the z coordinate inside the reactor, the latter is a description of the gas motion and reactions inside the spheres. For the gaseous bulk we will write one-dimensional conservation equations, for mass (of the different chemical species), energy and momentum of gas. We will take into account the mass and energy accumulation and convective transport terms (Froment and Bischoff, 1990; Bird *et al.*, 1960) and neglect the axial diffusion terms. In those equations, mass and energy transversal fluxes towards and from the spheres are also taken into account; these fluxes coincide with the corresponding fluxes (on the spheres surface) in the catalyst region model. For the catalyst region, we will consider the mass, energy and momentum conservation equations in the sphere radial coordinate R, with the accumulation, transport and diffusion terms. Thermal energy accumulation is considered in the solid phase only (energy accumulation is the gaseous phase is assumed to be negligible); thermal energy is transferred to the sphere outer surface by diffusion in the solid phase.

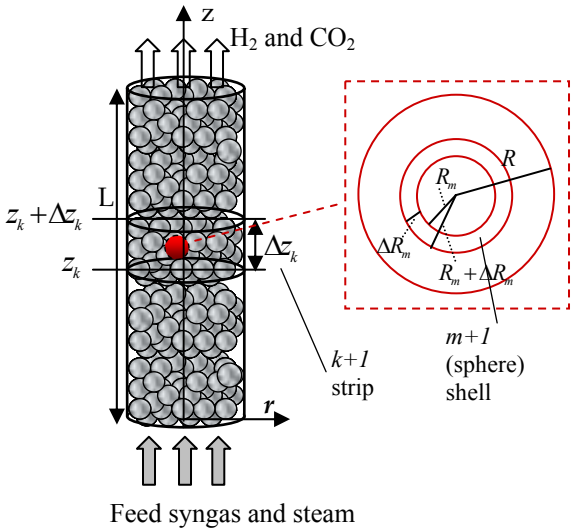

Fig. 1. A WGS reactor: model structure, based on strips and spheres (spheres represent the catalyst elements)

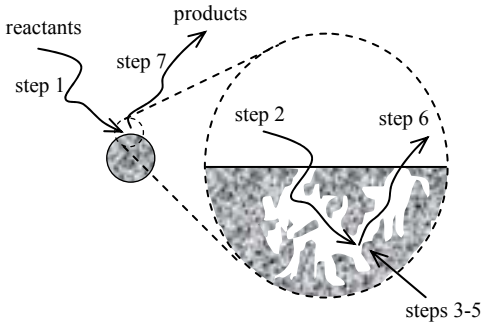

Fig. 2. The seven reaction steps on a catalytic element in a WGS reactor

Mass conservation. Mass conservation can be expressed, in the bulk and in the catalyst respectively, as follows.

- *Bulk:*

$$\frac{\partial(\rho_g \varepsilon_{g,b} A f_j)}{\partial t} + \frac{\partial(w_g f_j)}{\partial z} = h_{d,j}\Omega_c (f_{j,R_0} - f_j) - w_l' \Delta f_j \,, \quad (1)$$

where $\Delta f_j = f_j$ if $w_l' \geq 0$, $\Delta f_j = f_{j,R_0}$ if $w_l' < 0$. f_j is the generic j-th component bulk mass fraction, while f_{j,R_0} is the j-th component mass fraction at the outer surface of the catalyst pellets; w_g is the total axial mass flow rate, w_l' is the convective mass flow rate per unit length from the bulk to the catalyst pellets. At steady state, w_l' vanishes. $h_{d,j}$ is the diffusion coefficient between the bulk and the outer surface of the catalyst pellets; this outer surface, per unit length, is

indicated by Ω_c. A is the reactor total cross section, $\varepsilon_{g,b}$ the void fraction, ρ_g the bulk gas density. Of course, the terms on the left-hand side of (1) represent component j storage in the bulk and its convective transport along the z direction.

- *Catalyst:*

$$\frac{\partial(4\pi R^2 \tilde{C}_j)}{\partial t} + \frac{\partial(\tilde{w}_l \tilde{C}_j)}{\partial R} = \frac{\partial\left(4\pi R^2 D_j \frac{\partial \tilde{C}_j}{\partial R}\right)}{\partial R} + 4\pi R^2 \dot{r}_j(R,t), \quad (2)$$

where $\tilde{C}_j(R,t)$ is component j molar concentration and $\tilde{w}_l$ the convective molar flow rate at the surface of the sphere (of radius R). The two terms on the left-hand side of (2) have the same meaning as the corresponding terms in (1), only they are in the catalyst sphere radial direction. The first term on the right-hand side of (2) represents the j-th species diffusion in the radial direction (D_j (m^2/s) is the diffusion coefficient of component j in the porous medium, *i.e.* in the catalyst), while the second term represents the j-th reaction rate (it is the chemical generation or consumption term). The explicit expressions of the single chemical rates are the following ones:

$$\dot{r}_{CO} = k_{ri}(T)(1-\vartheta_{H_2O})\vartheta_{H_2} x_{CO_2} - k_{rd}(T)\vartheta_{H_2O} x_{CO} \quad (3)$$

$$\dot{r}_{H_2O} = -k_{ads}(T)(1-\vartheta_{H_2O}) x_{H_2O} + k_{des}(T)\vartheta_{H_2O} \quad (4)$$

$$\dot{r}_{CO_2} = -k_{ri}(T)(1-\vartheta_{H_2O})\vartheta_{H_2} x_{CO_2} + k_{rd}(T)\vartheta_{H_2O} x_{CO} \quad (5)$$

$$\dot{r}_{H_2} = -k_{dH_2}(T)(x_{H_2} + \vartheta_{H_2}) - k_{ri}(T)(1-\vartheta_{H_2O})\vartheta_{H_2} x_{CO_2} + \\ + k_{rd}(T)\vartheta_{H_2O} x_{CO} \quad (6)$$

where x_j is component j molar fraction and $T(R,t)$ is the catalyst temperature; subscripts *ri*, *rd*, *ads* and *des* for the k parameters refer to the reverse reaction, the direct reaction, the adsorption and the desorption process respectively; the meaning of the ϑ_{H_2O} and ϑ_{H_2} variables and of k_{dH_2} is illustrated in Section 3.2.

Energy conservation. As for energy equations, we have the following ones.

- *Bulk:*

$$\frac{\partial\left(\rho_g A e_g\right)}{\partial t} + \frac{\partial\left(w_g h_g\right)}{\partial z} = \frac{\partial\left(\lambda_g A \varepsilon_{g,b} \frac{\partial T_g}{\partial z}\right)}{\partial z} + \gamma_{cg}\Omega_c(T - T_g) \quad (7)$$

where e_g is the bulk gas specific energy, h_g its specific enthalpy and T_g its temperature; λ_g is the thermal energy diffusion coefficient in the axial direction, γ_{cg} is the heat transfer coefficient between the sphere outer surface and the fluid in the bulk. On the left-hand side of (7), if course, there are the accumulation and transport term, while on the right-hand side the axial diffusion term and the exchange term between gas and the catalyst material.

- *Catalyst:*

$$\frac{\partial(4\pi R^2 C_c T)}{\partial t} = \frac{\partial\left(\lambda_c 4\pi R^2 \frac{\partial T}{\partial R}\right)}{\partial R} + 4\pi R^2 H_{0,react}\dot{r} \quad (8)$$

where C_c is the thermal capacity per unit volume, λ_c the thermal energy diffusion coefficient in the radial direction, $H_{0,react}$ the standard reaction enthalpy, $\dot{r}$ the total reaction rate. From left to right, respectively, one can find the energy accumulation term, the diffusion term and the chemical generation term.

Momentum conservation. The equation to consider can be written as

$$\frac{\partial w_g}{\partial t} + \frac{\partial \frac{w_g^2}{\rho_g A}}{\partial x} = -A\frac{\partial p_g}{\partial x} - F'_{fr}, \quad (9)$$

where p_g is the bulk gas pressure and F'_{fr} is the friction force per unit length. On the left-hand side, there are the inertial terms of course.

3.2 Kinetic-chemical equations

The main components in the inlet syngas are H_2O, CO_2, CO, N_2 and H_2. In order to decrease model complexity, and following (Podolski and Kim, 1974), we assume that adsorption and desorption on the catalyst surface occur for water steam and for hydrogen only.

Denote by ϑ_{H_2O} (ϑ_{H_2}, respectively) the H_2O (H_2) *occupation ratio*, *i.e.* the ratio between the active site surface occupied by H_2O (H_2) and the active site surface still available; in other words, ϑ_{H_2O} (ϑ_{H_2}, respectively) is the total active *surface fraction* occupied by H_2O (H_2), such that $0 \le \vartheta_{H_2O} \le 1$ ($0 \le \vartheta_{H_2} \le 1$). The actually free surface is $1 - \vartheta_{H_2O} - \vartheta_{H_2}$. The conservation equations describing the kinetic-chemical behaviour of the analyzed system (compare Langmuir's studies reported in Froment and Bischoff, 1990) are

$$\tau_{H_2O}\frac{\partial \vartheta_{H_2O}}{\partial t} = k_{ads}(T)(1-\vartheta_{H_2O})x_{H_2O} - k_{des}(T)\vartheta_{H_2O} + \\ + k_{ri}(T)(1-\vartheta_{H_2O})\vartheta_{H_2} x_{CO_2} - k_{rd}(T)\vartheta_{H_2O} x_{CO} \quad (10)$$

$$\tau_{H_2}\frac{\partial \vartheta_{H_2}}{\partial t} = k_{dH_2}(T_i)(x_{H_2} - \vartheta_{H_2}), \quad (11)$$

where τ_{H_2O} and τ_{H_2} are, of course, the time constants for the transient behaviour of variables $\vartheta_{H_2O}(R)$ and $\vartheta_{H_2}(R)$, and $T(R)$ is the *local* temperature inside the sphere.

In (10), in particular, there are an adsorption term, which is proportional to the catalyst free surface and to the steam molar fraction in the mixture (this is a positive term, since it increases the surface fraction occupied by water); a desorption term, which is proportional to the surface occupied by steam (this is negative, since, when a component is desorbed, it decreases the occupied surface); an inverse reaction term, which is proportional to that amount of surface which is left free by water, to the surface occupied by

hydrogen and to CO_2 molar fraction (this term is positive, in that, if the inverse shift reaction occurs, the reactants concentration increases, therefore, apart from a proportionality coefficient depending on temperature, the surface occupied by water steam increases as well); a direct reaction term, which is proportional to the surface occupied by H_2O and to CO molar fraction in the mixture (this is negative, since, if the direct reaction occurs, the reactants concentration decreases, so the surface occupied by steam decreases too).

As for (11), the catalyst surface occupied by hydrogen increases, thanks to a weighting coefficient k_{dH_2}, when the concentration of hydrogen increases. The minus sign in the right-hand side parentheses is related to the fact that, when more active surface is occupied by hydrogen, the inverse reaction is more likely to occur.

Of course, both adsorption and desorption terms depend on local temperature, pressure and component molar concentrations x_j.

3.3 The global model: implementation issues

Summing up, the global model is constituted by a set of nonlinear partial differential equations, namely by the mass, energy and momentum conservation equations and by the kinetic-chemical equations. The two families of equations are linked together, for example, by the reaction rates (3-6), which are included in the mass equations and, at the same time, are expressed as functions of the chemical ϑ variables.

As far as numerical resolution is concerned, the distributed-parameter equations just described have been integrated along their own spatial dimension, *i.e.* along coordinate z or R (see Figure 1). More precisely, as shown in Figure 1, the cylindrical reactor can be divided, first of all, into a number of control volumes, here called *strips*, along its axial coordinate. A strip is just a section of the shift reactor cylinder, from coordinate z_k to $z_k+\Delta z_k$. Each strip, in turn, contains a number of spheres of adsorbing material, each of which is divided into a number of elementary shells (each one of thickness ΔR_m, between coordinate R_m and $R_m+\Delta R_m$), so as to model possible inhomogeneous ad-de-sorption and reaction inside it and therefore a possible inhomogeneous catalytic activity (this inhomogeneity is negligible, anyway, if a sphere is small enough). Here, for simplicity, we assume that all strips have the same thickness and we take as a reference an ideal, typical, average sphere, with fixed radius, fixed porosity coefficient and only one shell.

In particular, the thermo-fluid-dynamical equations have been integrated strip by strip, so that they become ordinary differential equations in each strip, while the kinetic-chemical equations are already written strip by strip, since they concern the sphere which is in the strip.

The obtained lumped-parameter equations have been discretized along the time coordinate according to the implicit Euler method; finally, a standard iterative linearization algorithm has been adopted to obtain the evolution of the unknowns. This procedure has been implemented in the Matlab-Simulink environment, by means of S-functions written in the C programming language: a reactor is simulated by the interaction of thermal, kinetic-chemical and fluid-dynamical S-functions.

We do not report the obtained lumped-parameter equations, for brevity. We just observe that the momentum conservation equation (9) has been integrated along the whole reactor length, neglecting the inertial term and using, for the friction term, the Ergun correlation (Bird, *et al.*, 1960), so that the reactor inlet mass flow rate w_{ing} can be expressed as a function of the pressure difference $p_{ing} - p_b$ between the reactor inlet and outlet:

$$w_{ing} = \frac{2(p_{ing}-p_b)\rho_g A^2 \frac{D_0}{L}\frac{\varepsilon_{g,b}^2}{(1-\varepsilon_g^2)}}{d^2 + \left[d^2 + 4(p_{ing}-p_b)\rho_g A^2 \frac{D_0}{L}\frac{\varepsilon_{g,b}^2}{(1-\varepsilon_g^2)}1.75 \right]^{\frac{1}{2}}}$$

$$d = 150(1-\varepsilon_{g,b})\mu_g A D_0 \qquad (12)$$

Integrating the overall mass flow rate (of all the species) along the whole reactor length, the differential equation of the reactor outlet pressure can be obtained.

It is worth to point out that the convective radial mass flow rate w_l has been neglected (of course, it is surely null in steady state conditions), and that the axial mass flow rate has been assumed as linear between the inlet and outlet mass flow rates.

4. PARAMETER ESTIMATION AND MODEL VALIDATION

The conceptual core of the single shift reactor model presented so far is the kinetic-chemical behaviour description. To obtain a reliable description, the estimation of the kinetic parameters k_{ads}, k_{des}, k_{ri}, k_{rd} is crucial. Here, the identification problem has been tackled as follows.

4.1 The reaction rate

By adding all single component rates given in (3-6), the "total rate" $\dot{r}$ can be found:

$$\dot{r} = k_{rd}(T)\vartheta_{H_2O}x_{CO} - k_{ri}(T)(1-\vartheta_{H_2O})\vartheta_{H_2}x_{CO_2} \qquad (13)$$

Considering (11) and (12) at steady state, one can obtain ϑ_{H_2O} and $1-\vartheta_{H_2O}$, which can be substituted into (13) to get

$$\dot{r} = \frac{\frac{k_{rd}(T)k_{ads}(T)}{k_{des}(T)}\left(x_{CO}x_{H_2O} - \frac{1}{K_{eq}}x_{H_2}x_{CO_2} \right)}{1 + \frac{k_{ads}(T)}{k_{des}(T)}x_{H_2O} + \frac{k_{rd}(T)}{k_{des}(T)}x_{CO} + \frac{k_{ri}(T)}{k_{des}(T)}x_{H_2}x_{CO_2}} \qquad (14)$$

(expressed in kmol/(m^2 of catalyst · s)). Here,

$$K_{eq} := \frac{x_{H_2} x_{CO_2}}{x_{H_2O} x_{CO}} = \frac{k_{rd}(T) k_{ads}(T)}{k_{ri}(T) k_{des}(T)} \qquad (15)$$

is the global shift reaction equilibrium constant. We notice the rate model (14) is very similar to other models which can be found in the literature, such as the Langmuir-Hinshelwood model and the Eley-Rideal model (Podolski and Kim, 1974).

Experimental data series about the three temperature values T = 677 K, T = 654 K and T = 633 K can be found in (Podolski and Kim, 1974): for each temperature, they supply CO, H_2O, CO_2 and H_2 molar fractions values and the corresponding measured rate r, expressed in mol/(g of catalyst · min). A part of the (Podolski and Kim, 1974) data have been used here for parameter estimation, a part for model validation; we notice that the relation between rate $\dot{r}$ in (14) and the experimental rate r used in (Podolski and Kim, 1974) is $\dot{r} = r/(S_c \cdot 60)$, where S_c is the contact surface between catalytic medium and gas per unit mass (m^2/g). At the three considered temperatures, K_{eq} takes on these values (Sandler, 1989):

$$K_{eq}(677\ \text{K}) = 11.22,$$

$$K_{eq}(654\ \text{K}) = 14.29,$$

$$K_{eq}(633\ \text{K}) = 18.07.$$

4.2 The identification procedure

Let us now describe the identification procedure adopted here. We refer to the nonlinear relation

$$y = f(\overline{u}, \overline{K}), \qquad (16)$$

where $\overline{u}$ is a vector input, y a scalar output and $\overline{K}$ a parameter vector. The aim is to identify $\overline{K}$ thanks to a set of $(\overline{u}, y)$ data. In the present case, $\overline{u}$ is the various components (H_2O, CO, CO_2, H_2) molar fractions vector, *i.e.* $\overline{u} = [x_{H_2O}, x_{CO}, x_{CO_2}, x_{H_2}]$, and y is the reaction rate r, while $\overline{K}$ is the kinetic parameters vector, *i.e.* $\overline{K} = [k_{ads}, k_{des}, k_{ri}, k_{rd}]$. The k_is (i = *ads, des, ri, rd*), and therefore $\overline{K}$, are functions of the temperature; this is why, as anticipated in Section 4.1, data at (three) different temperatures are considered.

We notice that, in $\overline{K}$, only three elements are independent, since there is constraint (15).

For each temperature, we choose three independent experiments and then solve for the three unknown parameters in $\overline{K}$: thus we obtain a set of possible rough estimates for $\overline{K}$ ($\overline{K}$ must be positive) at that temperature. We then employ these values as a first guess in the minimization of the following cost function J:

$$J = \frac{1}{N_{experiments}} \sum_{i=1}^{N_{experiments}} \frac{|\hat{y}_i - y_i|}{y_i}, \qquad (17)$$

where $\hat{y}$ is the rate estimate obtained from the model with the previously estimated k_i's, while y is the experimentally measured rate r, in the considered conditions. We have found that the minimum of J was very close to the first guess, which supports model reliability.

Now, a well-known result in chemistry is that parameters k_i vary exponentially with temperature, *i.e.*

$$k_i(T) = K_{0,i} \exp\left(\frac{E_{0,i}}{R \cdot T}\right). \qquad (18)$$

In the present case, coefficients $E_{0,j}$ and $K_{0,j}$ which yield the best approximation to this exponential law in the considered temperature range (633 K - 677 K) have been determined. Correspondingly, parameters $\overline{K}$ vary with temperature as shown in Figure 3, where a star indicates those points where the estimate could be done, while the dashed line describes the approximated trend of the same parameters outside the considered temperature range (633 K - 677 K).

The parameter estimation average error is here

$$\overline{E} = \frac{1}{3} \sum_{\substack{T=633\,K,\\ T=654\,K,\\ T=677\,K}} \left(\frac{1}{N_{experiments}} \sum_{i=1}^{N_{experiments}} \frac{|\hat{y}_i - y_i|}{y_i} \right)_T, \qquad (19)$$

which is rather good, since it amounts to 7.49 %.

4.3 Model validation

Finally, we present some results obtained from a steady-state validation carried out thanks to experimental data (see Table 1, Radaelli and Savoldelli, 2005), referred to a laboratory-scale shift reactor located at CESI RICERCA laboratory in Milan. That 700 mm long reactor has a 76.5 mm diameter, with 2900 cm^3 maximal useful volume; its maximal working temperature and pressure are 773 K and 5 bar.

The first three conditions in Table 1 are characterized by different spatial velocities (the spatial velocity is the reciprocal of the depletion time of the empty reactor, *i.e.* the syngas mass flow rate divided by the syngas mass inside the reactor) and by steam/CO molar ratios nearly constant (around 3), the subsequent two by the same spatial velocity and by different steam/CO molar ratios, the last three by different spatial velocities and by different steam/CO molar ratios. Comparison between the experimental values and those calculated by the proposed model shows substantially good matching.

We notice that the conversion values in Table 1 are not so far from the equilibrium values, but they are not exactly the equilibrium ones; this has allowed for the identification of the diffusion coefficients D_j's (of the various components),

which have been assumed to be related mainly to the characteristics of the porous medium and have then been identified so as to minimize the error with respect to the temperature.

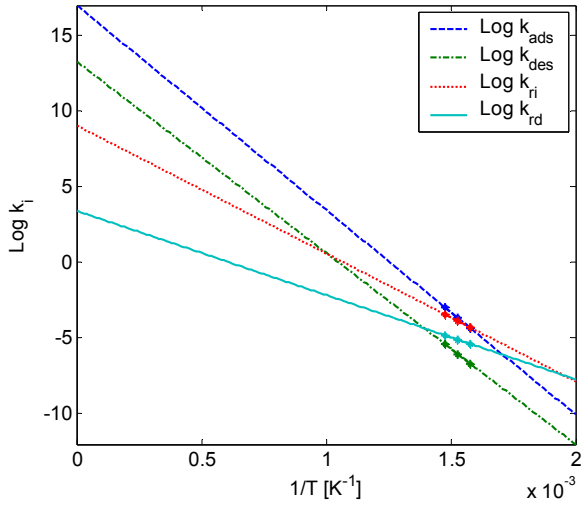

Fig. 3. The estimated kinetic coefficients

5. SIMULATION RESULTS

The simulator has been employed to test the model behaviour in different operating conditions. We remind that the model supplies dynamical temperatures and molar fractions not only in the strips, but also in the spheres; mass and heat exchanges between bulk and porous surfaces, anyway, are so efficient that differences between quantities in a strip bulk and in the corresponding sphere are very light: for this reason, we do not report numerical results for variables inside spheres.

Let us consider the laboratory reactor, with 1.4 mol/s syngas inlet flow rate and inlet molar fractions amounting to 0.5592 for H_2O, 0.1907 for CO, 0.0755 for CO_2 and 0.1619 for H_2, and the syngas inlet temperature 638 K.

By dividing it into four strips, the spatial distribution of bulk molar fractions and temperatures which is reached at steady state is shown in Figure 4; none of these variables are uniform in any strips, namely the chosen conditions do not lead either to chemical equilibrium or to thermal equilibrium. We observe that the expected behaviour is highlighted in the simulation, in that as temperature increases spatially, bulk CO and H_2O molar fractions have decreasing values, and bulk H_2 and CO_2 molar fractions have increasing values.

As far as dynamical simulations are concerned, we just observe that fluid-dynamic and thermal time constants are rather similar, ranging from about half a minute to around 1.5 minutes; this is due to the fact that chemical reactions generate heat directly inside the porous medium, in a uniform way beside, and heat leaves the exchange surface rather easily and fast, since such surface is very large, due to high porosity.

Table 1. Validation in steady-state conditions; different colours separate different trial sets; v is the space velocity

Reactor inlet (Radaelli and Savoldelli, 2005)			Reactor outlet		Simulation results	
v (h^{-1})	H_2O/CO ratio R	T (K)	T *max* (K)	*CO* % molar conversion	T *max* (K)	*CO* % molar conversion
2000	2.93	638	725	90.8	725.01	90.63
3000	3.03	659	756	89.8	756.89	89.62
4000	2.82	656	758	87.1	758.75	88.14
1000	10.91	610	652	97.2	652.18	94.99
1000	4.12	589	719	95.0	721.65	95.34
2000	5.08	589	648	91.7	649.55	90.75
3000	3.93	629	669	88.7	666.34	88.82
4000	4.28	654	675	86.9	675.4	86.15

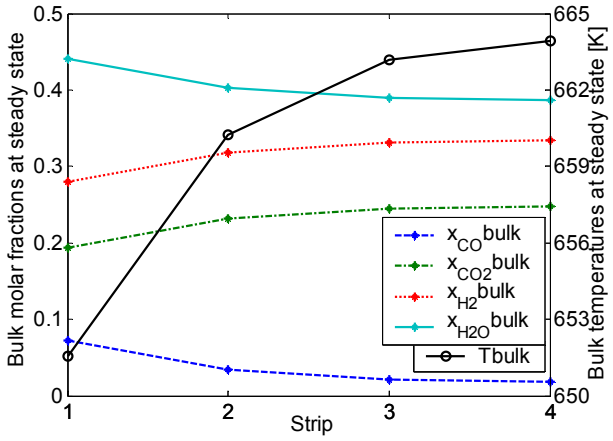

Fig. 4. Bulk steady-state variables along the reactor

Finally, it is interesting, for example, to analyze how the reactor behaviour is affected when chemical composition is changed, while keeping the inlet mass flow rate constant (this because a flow rate variation would mask all other effects). Let us consider, in particular, the effects of large step variations of the inlet steam molar fraction: starting from the previously found steady state, at time t = 1200 s the inlet H_2O molar fraction is given a 50 % positive step, from 0.5592 to 0.8388, and then, after a new steady state has been reached, an identical negative step (around time t = 4200 s); accordingly, in order to keep the sum of all inlet molar fractions equal to 1, the other inlet molar fractions are first reduced and then increased by a factor λ = 0.3657. The time behaviour of the various components molar fractions and temperature in the last strip, *i.e.* at the reactor outlet, is depicted in Figures 5 and 6. Thanks to the large steam addition, CO conversion passes from 90.61 % to 98.85 %, as expected.

6. CONTROL ISSUES

The model has been validated in steady-state conditions for a laboratory-scale reactor, but, of course, it can be used for simulation of industrial-scale shift reactors as well.

It has already been pointed out that this dynamical model has been developed in order to study different control strategies for the shift reactor.

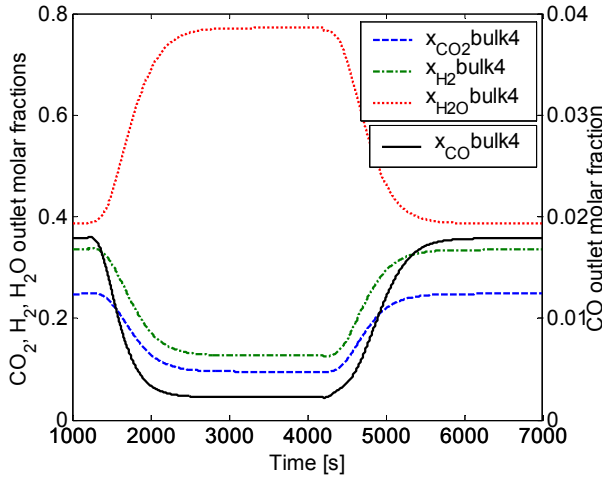

Fig. 5. Bulk molar fractions at the reactor outlet, *i.e.* at strip 4

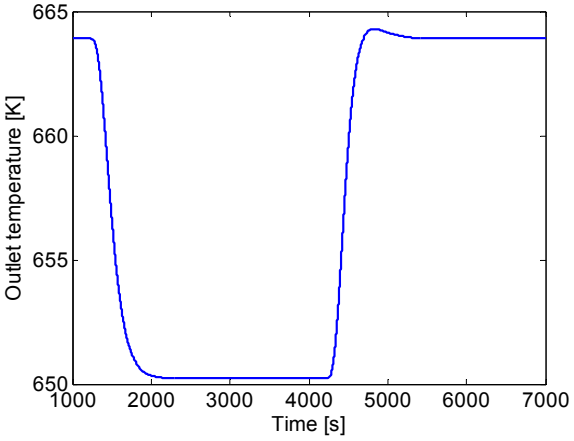

Fig. 6. Bulk temperature at the reactor outlet, *i.e.* at strip 4

First of all, the shift reaction is strongly exothermal, so the temperature inside the reactor increases; furthermore, the catalyst has its own operating temperature range, so generally the shift conversion is realised with two or more reactors in cascade, with a suitable heat exchanger in between them in order to cool the syngas with *partial* CO conversion. It is clear that the control problems of these reactors and of the cooling heat exchangers are to be investigated together.

Another issue is that the reaction of CO conversion is shifted towards H_2 production by injecting H_2O steam into the syngas, so the ratio between steam flow and CO_2 flow has to be constrained as well (in relation also with temperatures) in order to avoid the formation of carbon black.

Furthermore the inlet temperature, mass flow rate and composition of the syngas, related to the upstream coal gasification process, are disturbances which have to be considered. The control of the shift reactor has to be integrated with the control of the whole plant. For this reason, an overall simulation model of the whole plant is needed, integrating the gasification process with the shift reactor.

7. CONCLUSIONS

A dynamical model for a shift reactor converting carbon monoxide into hydrogen has been developed. This description is based on first principles, namely on mass, momentum and energy conservation equations.

Model validation at steady state was carried out thanks to experimental data about a laboratory reactor, while unknown parameters were tuned by means of literature experimental data and by the test data themselves; steady-state and dynamical simulations were carried out for that reactor.

Future activities include, first of all, model validation in transient conditions and integration between this model and a model of the upstream gasification plant; then, control strategies will be studied concerning the shift reactor itself and/or the interaction between the reactor and the other devices in the gasification plant.

8. ACKNOWLEDGMENTS

This work has been financed by the Research Fund for the Italian Electrical system under the Contract Agreement between CESI RICERCA and the Ministry of Economic Development - General Directorate for Energy and Mining Resources stipulated on June 21, 2007 in compliance with the Decree n. 73 of June 18, 2007. Research has also been supported by the Italian National Research Project "New Techniques of Identification and Adaptive Control for Industrial Systems" and partially by CNR-IEIIT.

REFERENCES

Bird, R.B., W.E. Stewart and E.N. Lightfoot (1960). *Transport phenomena*. John Wiley & Sons Inc., New York.

Fantini V., L. Mazzocchi, F. Moia, V. Prandoni and P. Savoldelli (2007). Pre-feasibility Study of a Flexible Hydrogen-Electricity Co-production IGCC Coal-fed Plant with CO_2 Capture and Sequestration. Third International Conference on Clean Coal Technologies for our Future (CCT) 2007, 15-17 May, Cagliari, Italy.

Froment, G.F. and K.B. Bischoff (1990). *Chemical reactor analysis and design* (Second Edition). John Wiley Series in Chemical Engineering, New York.

Ogden, J.M. (1999). Hydrogen energy systems studies. In: *Proceedings of the 1999 U.S DOE Hydrogen Program Review*. Available at http://www1.eere.energy.gov.

Podolski, W.F. and Y.G. Kim (1974). Modeling the Water-Gas Shift reaction. *Ind. Eng. Chem.*, **13**, no. 4, pp. 415-421.

Radaelli, M. and P. Savoldelli (2005). Sperimentazione di laboratorio del processo WGS con syngas prodotto con la tecnica POR e da gassificazione del carbone. Available at http://www.ricercadisistema.it.

Sandler, S.I. (1989). *Chemical and engineering thermodynamics* (Second Edition). Wiley Series in Chemical Engineering, John Wiley & Sons, New York.

Yoon, H.C. and P.A. Erickson (2005). Hydrogen from Coal-Derived Methanol: Experimental Results. *AIAA, 3rd International Energy Conversion Engineering Conference*, 15-18 August 2005, San Francisco, California, USA.